(π^+, pp) reaction on several light nuclei*

E. D. Arthur†
University of Virginia, Charlottesville, Virginia 22901

W. C. Lam‡
Carnegie-Mellon University, Pittsburgh, Pennsylvania 15213

J. Amato§
Los Alamos Scientific Laboratory, Los Alamos, New Mexico 87544

D. Axen
University of British Columbia, Vancouver, British Columbia, Canada

R. L. Burman
Los Alamos Scientific Laboratory, Los Alamos, New Mexico 87544

P. Fessenden
Oregon State University, Corvallis, Oregon 97311

R. Macek, J. Oostens,‖ and W. Shlaer
Los Alamos Scientific Laboratory, Los Alamos, New Mexico 87544

S. Sobottka
University of Virginia, Charlottesville, Virginia 22901

M. Salomon
University of British Columbia, Vancouver, British Columbia, Canada

W. Swenson
Oregon State University, Corvallis, Oregon 97311
(Received 1 July 1974)

The $(\pi^+,2p)$ reaction has been studied on targets of ^{2}H, ^{6}Li, ^{14}N, and ^{16}O with 70-MeV pions. All kinematical quantities needed to define completely the final state were determined. The data are presented in an unbiased form, integrated over well-defined regions in phase space, and are thus readily comparable with available theoretical calculations. Data were obtained for opening angles both on and off the kinematics of the free process, $\pi^+ + d \rightarrow p + p$. Thus a more extensive test of the applicability of a pole model or impulse approximation which assumes absorption on a quasideuteron could be made. For ^{6}Li and ^{16}O the center of mass angular distribution was determined and compared with that for π^+ absorption on a free deuteron. Nuclear structure effects appear to play an important role for capture on ^{16}O and ^{14}N, since little excitation of the low-lying levels of the residual nuclei was observed, in contrast to theoretical predictions. For events leading to low excitation of the residual nucleus, theoretical curves in recoil and relative momentum, Treiman-Yang angle, and opening angle calculated for a pole model or plane wave impulse approximation gave general agreement with the measured distributions even for events off the kinematics of the free πd process.

[NUCLEAR REACTIONS ^{2}H, ^{6}Li, ^{14}N, ^{16}O(π^+, pp), $E = 70$ MeV, measured $\sigma(E_1, E_2, \theta_1, \theta_2)$.]

I. INTRODUCTION

The dominant mode for pion absorption is capture upon two closely correlated nucleons. The high relative momentum of the two outgoing nucleons indicates that very small distances can be probed (<0.5 fm), and the reaction has been suggested as a means to obtain information concerning short-range correlations in the initial nucleus.[1,2] Two-hole shell model nuclear states can also be studied using this reaction.

Theoretical calculations[3-13] of the (π, NN) process have been made assuming the two-nucleon capture mechanism. Information concerning short-range correlations is masked to some extent by complications resulting from final state interactions between the two outgoing nucleons. Final state interactions have been included in various calculations

through the use of the asymptotic form of the nucleon-nucleon scattering amplitudes,[3,4] and through the solution of the Schrödinger equation for the motion of two particles in a realistic potential.[5,6] Further complications arise from interactions between the outgoing nucleons and the residual nucleus (nuclear distortions). For the most part, the latter effect has been neglected; exceptions are the calculations of Kaushal and Waghmare[12] and those of Morris and Weber[13] for the (π^-, NN) process on ^{12}C.

The simplest description of the (π, NN) process is through the use of the pole model or impulse approximation.[14,15] In particular, for the (π^+, pp) reaction, the cross section for absorption on a complex nucleus is proportional to the cross section for absorption on a free deuteron. The reaction is thus dominated by the kinematics for the process

$$\pi^+ + d \rightarrow p + p \,. \tag{1}$$

Initial and final state interactions are neglected except for effects included in the cross section for the elementary process (1). Previous experimental measurements of the (π^+, pp) reaction on light nuclei[16-18] were interpreted using this model. Good agreement[17] was obtained between the experimental data and theoretical predictions for ^6Li. However, results were presented uncorrected for geometrical bias, so that comparison with theory could only be accomplished after integration over the particular geometry of the experimental apparatus.

Our experiment sought to test further the applicability of this model by extending the kinematical range over which data were acquired and by improving the energy resolution. The energy and direction of the outgoing protons were measured, and thus all the kinematical variables needed to define completely the final state were determined. We present in this paper the results of our measurements of the (π^+, pp) process on ^2H, ^6Li, ^{14}N, and ^{16}O. Data were taken at opening angles equal to the free deuteron angle of reaction (1), but which had different c.m. angle values. Data were also obtained at opening angles off the free deuteron angle. All three-body final state data have been corrected for geometrical effects and are thus in a form readily comparable with available theoretical calculations.

II. THEORETICAL BACKGROUND–THE PLANE WAVE IMPULSE APPROXIMATION

The three-body problem of the (π^+, pp) reaction on a complex nucleus is reduced using the plane wave impulse approximation (PWIA) to the equivalent two-body reaction of π^+ absorption on a quasideuteron. The diagram for the process is shown in Fig. 1 where $\vec{p}_\pi, \vec{p}_A$, and $\vec{p}_B$ are the momenta of the incoming pion and the ejected protons, $\vec{p}(A, Z)$ is the momentum of the target nucleus (zero in the laboratory system), p_R is the momentum of the recoiling $A-2$ system which may be bound or unbound, and $\vec{p}_{np}$ is the momentum of the virtual np pair. To derive a cross section expression with the PWIA, the following assumptions are made:

(a) The wave function for the target nucleus can be represented schematically by

$$\psi_A \sim \psi_{A-2}\psi(\vec{R}_d - \vec{R}_{A-2})\psi_d \,. \tag{2}$$

Here ψ_{A-2} is the wave function of the residual $A-2$ system, ψ_d is the internal wave function of the quasideuteron, and $\psi(\vec{R}_d - \vec{R}_{A-2})$ describes the relative motion between these two clusters.

(b) Plane waves represent the incoming pion and outgoing protons.

(c) Absorption is considered to take place on a quasideuteron with the residual system acting as a spectator for the reaction. In this approximation the momentum of the np pair before capture is equal and opposite to that of the $A-2$ system. If the PWIA is valid, measurement of the distribution of recoil momentum $\vec{p}_R$ will give the momentum distribution of the quasideuteron in the target nucleus.

(d) The quasifree approximation is used; i.e., the cross section for absorption upon a quasideuteron bound within the initial nucleus is considered to be the same as that for absorption on a free deuteron.

With these conditions the PWIA form for the (π^+, pp) cross section is given by[19]

$$d\sigma = N_d |\phi(\vec{p}_R)|^2 \left(\frac{d\sigma}{d\Omega}\right)_d \frac{p'_\pi}{p'} \frac{\omega^2}{m_d p_n} \times \frac{p_A p_B dT_A d\Omega_A d\Omega_B}{|1 - \vec{V}_R \cdot \vec{V}_B / V_B^2|} \,. \tag{3}$$

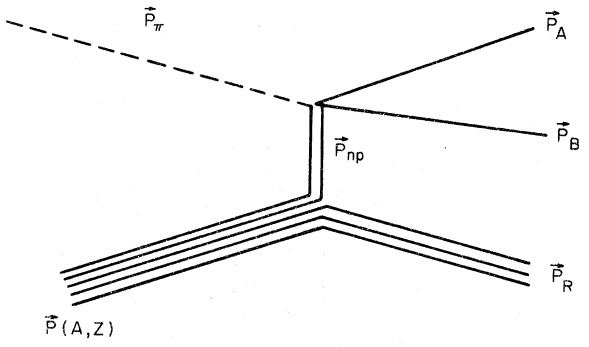

FIG. 1. Pole model diagram for the $(\pi^+, 2p)$ reaction.

Defined in the c.m. of the ejected protons are the magnitudes of the pion and proton momenta, p'_π and p', the sum ω of the total energies of the protons, and $(d\sigma/d\Omega)_d$, the differential cross section for the free process (1). The term $\phi(p_R)$, with the integral of the absolute value squared normalized to unity, is the Fourier transform of the wave function which describes the relative motion of the clusters. The quantities $\vec{V}_B$ and $\vec{V}_R$ which appear in the phase space term of Eq. (3) refer to the velocities of one of the outgoing protons and the recoiling nucleus, respectively.

The factor N_d is the effective number of deuterons in the target nucleus and is defined by Eq. (3). It is related to the probability that a nucleus can be described in terms of a quasideuteron and some state (E, J, T) of the residual $A-2$ system. The effective number of deuterons N_d is obtained by a fit of Eq. (3) to our experimental data.

Favier *et al.*[17] have used an expression for the cross section based on the pole model for the reaction. This expression appears below and exhibits explicitly a pole term, $(p_R{}^2+\alpha^2)$, in the denominator

$$d\sigma = \frac{N_d}{\pi^2}\frac{\alpha}{m_d}\frac{|F(p_R)|^2\omega^2}{p_\pi(p_R{}^2+\alpha^2)^2}\frac{p'_\pi}{p'}\left(\frac{d\sigma}{d\Omega}\right)_d \frac{p_A p_B dT_A d\Omega_A d\Omega_B}{|1-\vec{V}_R\cdot\vec{V}_B/V_B^2|}\,. \tag{4}$$

The quantity α is related to the binding energy of a deuteron in the target nucleus

$$|E| = \frac{\hbar^2\alpha^2}{2M}\,, \tag{5}$$

where the reduced mass M is given by

$$\frac{1}{M} = \frac{1}{m_d} + \frac{1}{M_{A-2}}\,. \tag{6}$$

Favier *et al.*[17] define the form factor $F(p_R)$, which describes the motion of the virtual np pair and is related to the Fourier transform of the relative motion wave function, by

$$|F(p_R)|^2 = (p_R{}^2+\alpha^2)^2\frac{\pi^2}{\alpha^2}|\phi(p_R)|^2\,. \tag{7}$$

$F(p_R)$ is normalized such that for s-wave motion in a δ-function potential $F(p_R)=1$. This arbitrary choice of normalization serves to make the PWIA cross section form given by Eq. (3) equivalent to the pole model form of Eq. (4).[20] All other quantities which appear in Eq. (4) have been defined previously in Eq. (3).

III. EXPERIMENTAL TECHNIQUE

The experimental arrangement used for these measurements has been briefly described in a previous paper.[21] A more detailed description will be given here. Pions were produced when the external proton beam of the Lawrence Berkeley Laboratory 184-inch cyclotron struck a copper production target. Particles emitted at an angle of 30° were swept by a bending magnet into the experimental setup shown in Fig. 2. A second bending magnet served as an analyzing magnet which was used to determine the momentum of the beam particles. The position of each particle was measured at the entrance of the analyzing magnet by the 16×4 element hodoscope C_1 and the spark chamber planes S_1–S_4. Spark chambers used in this experiment were of the magnetostrictive readout variety. The high-particle fluxes at the entrance of the bending magnet produced many multiple tracks in S_1–S_4 which were resolved by use of the hodoscope. The position and angle of the particle at the exit of the magnet were measured using spark chamber planes S_5–S_7. With this information transport matrices which traced the particle backwards through the magnet were used to determine its momentum. The central energy of the pion beam was 70 MeV. The beam intensity was 3×10^4 particles/second, of which 62 ± 5% were pions as determined from time-of-flight analyses.

When an event occurred in the target, the position and angle of the outgoing protons were measured with spark chamber planes S_8–S_{13}. Two sets of 1.6-mm plastic scintillators mounted on each arm, C_3–C_6, provided dE/dX information. The proton energy was measured with 130-mm-diam by 100-mm-thick NaI crystals selected for their uniformity in response across their volume. In order to minimize gain shift effects, the crystals and associated electronics were housed in temperature-stabilized environments. The threshold for proton detection (35 MeV) was determined by the material in front of the NaI counters. The thickness of the crystal was sufficient to stop protons of energy 183 MeV.

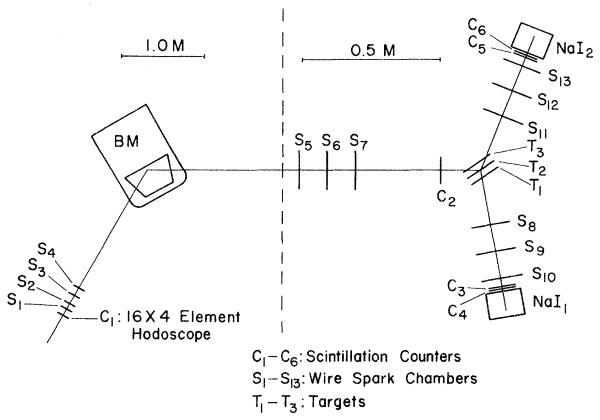

FIG. 2. Experimental geometry.

The information concerning the pion and proton directions allowed the determination of the reaction vertex to within 3 mm. In order to obtain an adequate event rate without undue degradation of energy resolution, we therefore used targets consisting of three sections separated by a distance of 29 mm. Events were assigned to a target section by the location of the vertex, and the energy loss of the outgoing protons in the remaining target sections was taken into account in calculating the proton energies.

Each event was processed by an XDS Sigma-2 computer which stored the event, and after the accumulation of several events, dumped them on magnetic tape. An on-line analysis program, operating in a background mode, calculated and displayed via histograms the kinematical and experimental parameters for each event. The performance of various experimental components was monitored through the use of a computer-controlled digital voltmeter.

The calibration of the NaI detectors, as well as the determination of the resolution in excitation energy, was obtained through measurement of π^+ absorption on deuterium. The resolutions in excitation energy and recoil momentum were 4.5 MeV [full width at half maximum (FWHM)] and 12 MeV/c (FWHM), respectively. A resolution of 1.6° (FWHM) was obtained in opening angle.

IV. DATA REDUCTION

A. Efficiency corrections and integration region definition

Experimental results presented in the following sections have been corrected for geometrical efficiencies and are thus in an unbiased form. Because of the geometrical complexity of the experimental apparatus, Monte Carlo methods were used to compute the acceptance. A uniform parent distribution was simulated in the apparatus, and the calculated distribution of detected events allowed the determination of the geometrical efficiency. To prevent large errors in the corrected data resulting from statistical errors in the computed acceptance, events occurring in regions for which the acceptance was less than 10 to 15% of the maximum were eliminated.

The cross sections obtained for the (π^+, pp) process depend on six kinematical quantities. In this experiment the set can be reduced to five since the range covered in pion energy is essentially constant. These quantities were chosen to be:
(a) θ_{AB}, the angle between the two emitted protons;
(b) θ_B, the angle of one proton with respect to the pion direction; and
(c) ϕ_B, the azimuthal angle of the same proton,

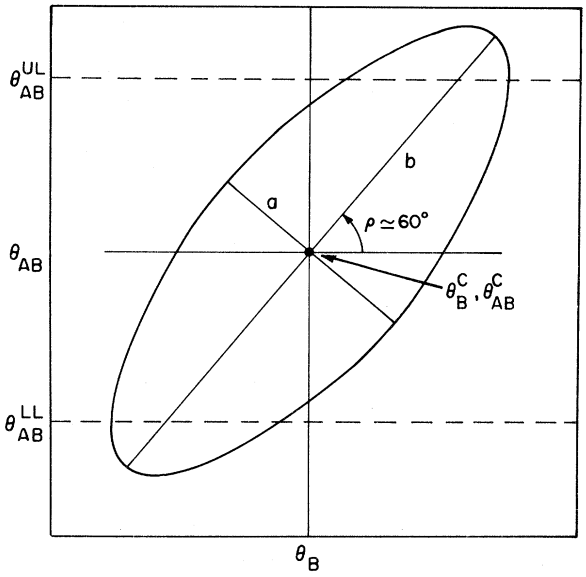

FIG. 3. Definition parameters used to described the truncated integration ellipses in the θ_{AB} versus θ_B plane.

defined as

$$\cos\phi_B = \frac{\vec{n}_A \cdot \vec{n}_B}{|\vec{n}_A||\vec{n}_B|}, \tag{8}$$

where $\vec{n}_A \equiv (\vec{p}_\pi \times \vec{p}_A)$ and $\vec{n}_B \equiv (\vec{p}_B \times \vec{p}_\pi)$;
(d) E_A and E_B, the energies of the two protons.

TABLE I. Integration region parameters for the ^{6}Li, ^{16}O, ^{14}N data.

Arm settings θ_A (deg)	θ_B (deg)	θ_B^C (deg)	θ_{AB}^C (deg)	a	b	θ_{AB}^{LL} (deg)	θ_{AB}^{UL} (deg)	ϕ_B (deg)
				^{6}Li				
38	98	98	136	3.9	26.5	110	158	±10
53	98	98	151	3.9	26.5	130	170	±10
63	98	98	161	3.9	26.5	140	180	±10
78	98	98	176	4.9	26.5	158	180	±10
80	80	78	156	4.1	24.7	143	176	±10
42	123	121	160	3.8	26.1	143	176	±10
				^{16}O				
25	113	113	138	3.9	26.1	118	156	±12
37.5	113	113	151	3.9	26.5	130	168	±12
50	113	111	160	3.9	23.9	140	176	±12
65	113	106	165	3.9	17.1	154	180	±12
80	113	106	175	4.1	10.2	164	180	±12
100	61	59.5	158	4.2	23.9	138	178	±12
				^{14}N				
57	105	105	162	4.2	24.4	140	178	±10

The experimental data will be presented as a function of a single variable after integration over a specified region in the remaining ones. To define the integration region over the quantities θ_{AB} and θ_B, truncated ellipses in the (θ_{AB}, θ_B) plane have been used. The construction of the ellipses, as defined in Fig. 3, was such that regions of poor geometrical efficiency were eliminated. The range of the azimuthal angle ϕ_B covered in this experiment was essentially constant. The apparatus settings in θ_A and θ_B for the ^{6}Li, ^{14}N, and ^{16}O targets, the pertinent parameters used to define each integration ellipse, and the range of ϕ_B are given in Table I. The use of θ_{AB} and θ_B leads to some ambiguity in θ_A, the angle of the first proton with respect to the pion direction. For a given θ_B, a cone defined by θ_{AB} is generated about θ_B, allowing two possible values for θ_A. We can define the angle which is the projection of θ_A on the π-θ_B plane. We have only used data for which the sum of this projected angle and θ_B is less than or equal to 180°, since only a small number of events did not satisfy this criterion.

The range for integration over the region of proton energies E_A and E_B covered in this experiment extends from the threshold for proton detection of 35 MeV up to 180 MeV.

B. Sources of error

To obtain cross sections, the data were corrected for spark chamber efficiencies, for the efficiency in reconstructing the event vertex, for the fraction of pions in the beam, and for the fraction of protons lost due to interactions in NaI crystals.[22,23] The errors, quoted for total cross sections obtained by integrating the data over the regions defined in Table I, are a combination of (1) statistical errors, (2) the errors associated with these correction factors, and (3) errors in the calculated acceptance function.

V. EXPERIMENTAL RESULTS

The influence of the absorption mechanism of Fig. 1 leads to characteristics in the experimental distributions which make this process readily identifiable. The most important characteristics are the following:

(a) Small values in recoil momentum are favored. Hence, events cluster around opening angles corresponding to the kinematics of the $\pi - d$ reaction.

(b) The cross section should exhibit the same dependence upon c.m. angle as the cross section for the free process (1).

(c) The cross section as a function of Treiman-Yang angle[24] will be isotropic if certain conditions for isotropy are defined. The Treiman-Yang angle is the angle between the plane defined by $\vec{p}(A, Z)$ and $\vec{p}_R$ (in the system for which $\vec{p}_\pi = 0$) and the plane defined by $\vec{p}_A$ and $\vec{p}_B$. As formulated by Shapiro,[25] isotropy in Treiman-Yang angle occurs when S_{np}, the spin of the transferred deuteron, is zero; when the quasideuteron and the residual nucleus are in an s state of relative motion (true for ^{6}Li); or when the channel spin $S_{np} + S_R$ is zero. Note that Eqs. (3) and (4) assume isotropy as a result of the factorization of the quantity $\phi(p_R)^2(d\sigma/d\Omega)_d$.

The experimental results will be presented so as to illustrate these effects and to point out deviations from them.

A. Deuterium results

A target of heavy water in a jellied form was used to investigate π^+ absorption on deuterium. Since our measurement of reaction (1) was overconstrained, we obtained a check on the performance of our experimental apparatus and an energy calibration for the NaI detectors. A Monte Carlo integration of the empirical differential cross section was made over our apparatus and was compared with the measured data. The cross section angular dependence was taken from Ref. 26, and has the form

$$\left(\frac{d\sigma}{d\Omega}\right)_{\text{c.m.}} = \frac{\sigma_{\text{tot}}}{2\pi} \frac{A + \cos^2\theta_{\text{c.m.}}}{A + \frac{1}{3}} , \tag{9}$$

where $\sigma_{\text{tot}} = 7.3 \pm 0.7$ mb and $A = 0.23 \pm 0.04$ for 70-MeV incident pions.

The comparison of the Monte Carlo results and the experimental data appears in Table II. The errors shown for the experimental and calculated cross sections are statistical. The agreement is satisfactory even for central arm angles not corresponding to free deuteron kinematics, for which the distribution of events across the targets is asymmetric.

TABLE II. Free-deuteron cross section results.

θ_A (deg)	θ_B (deg)	Measured value (μb)	Calculated value (μb)
50	113	2.94 ± 0.37	2.83 ± 0.2
100	61	1.98 ± 0.28	2.0 ± 0.15
65	113	1.09 ± 0.19	0.9 ± 0.1
37.5	113	1.95 ± 0.3	1.8 ± 0.13

B. ^{6}Li results

The $^6\text{Li}(\pi^+, pp)^4\text{He}$ reaction leads to the excitation energy spectra shown in Fig. 4 for opening angles θ_{AB} both on and off the kinematics for the free process. The structure evident in these spectra

has been observed previously in (π^+, pp) experiments,[16-18] in (π^-, nn) measurements,[27,28] and in the quasielastic (p, pd), ($p, p\alpha$), and ($\alpha, 2\alpha$) knockout reactions.[29-31] The dominant features are two peaks, the first of which results from capture leading to the ground state of ^{4}He. In a shell model description, capture on two weakly bound $p_{3/2}$ nucleons accounts for the existence of this peak. The second peak is then interpreted in terms of either capture on a ($1s, 1p$) pair or on a ($1s, 1s$) pair.

A cluster model explanation for this excitation energy spectrum has been advanced in a calculation performed by Golovanova and Zelenskaya.[32] In their interpretation, capture on a quasideuteron produces the events in the ground state peak; capture on a quasialpha or two nucleons in a quasialpha leads to excitation in the range greater than 25 MeV, and events in the region of 20 MeV result from capture on a pair of nucleons, one of which exists in the quasideuteron and the other in the quasialpha.

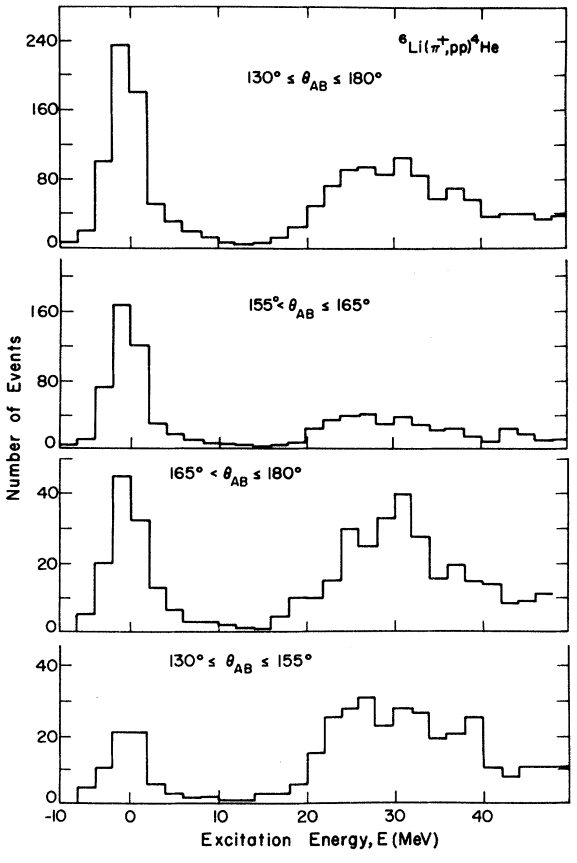

FIG. 4. Excitation energy spectra for ^{6}Li(π^+, pp)^{4}He events. Distributions are shown for regions of opening angles both on and off the kinematics ($\theta_{AB} \sim 162°$) for the free process, $\pi^+ + d \rightarrow p + p$.

In the full range of opening angles from 130° to 180° our ratio of ground state (−5 to 8 MeV excitation energy) to excited state events (20 to 40 MeV) is 0.67. This value agrees almost exactly with the value of 0.66 obtained by Golovanova and Zelenskaya[32] for the ratio of ground state to excited state events. For opening angles around that for the free process ($155° \leq \theta_{AB} < 165°$) we obtain a ratio of ground to excited state events of 1.22, whereas for off-deuteron angles ($130° \leq \theta_{AB} \leq 155°$ and $165° < \theta_{AB} \leq 180°$) we obtain ratios of 0.26 and 0.41, respectively.

1. Ground state results and interpretation

Events for the kinematics of the free process are characterized by low recoil momentum values, and as shown in Fig. 5, are located mostly in the ground state peak, with relatively little contribution from higher excitation energy events. To interpret the results for events in the ground state peak, we have followed the method of analysis used in Ref. 17, that is, we assume a cluster model representation for ^{6}Li and describe it in terms of an α particle and a deuteron in an s state of relative motion. The cross section for the process was given in Eq. (4) with the assumptions described in Sec. II. The empirical energy and angular dependence of the cross section $(d\sigma/d\Omega)_d$, for the free process of pion absorption on a deuteron, was based on the results of Rose[26] and of Richard-Serre *et al.*[33]

Several wave functions were used to represent the relative motion of the clusters, the first of which was the Hulthen wave function,

$$\psi(r) \propto (e^{-\alpha r} - e^{-\lambda r})/r . \qquad (10)$$

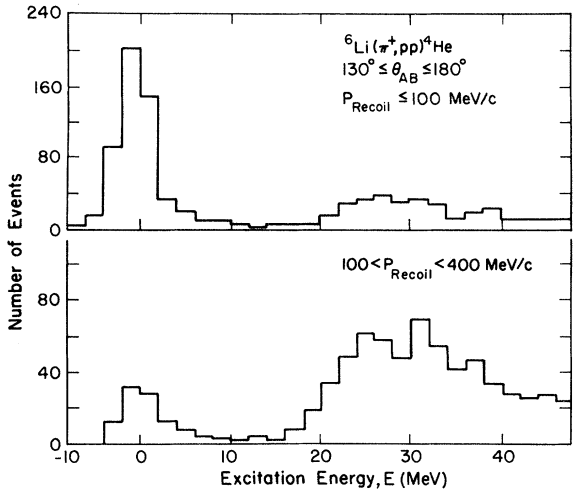

FIG. 5. Excitation energy distributions for ^{6}Li(π^+, pp)^{4}He events for regions of high and low recoil momentum.

Here $\alpha = 0.37$ fm^{-1} from Eq. (5), while the quantity λ is a parameter which can be adjusted to best fit the experimental data.

Two other wave functions were used to describe the relative motion of the clusters. The first was the cluster model wave function formulated by Tang, Wildermuth, and Pearlstein,[34] and used by several authors in the calculation of the ^{6}Li(π^-, nn)-^{4}He process,[35,36]

$$\psi(r) \propto r^2 e^{(-2/3)\beta r^2} . \tag{11}$$

The parameter β which appears in this expression is related to the oscillator width parameter, $\beta_0 = 0.44$ fm^{-2} for an α particle by

$$\beta = x\beta_0 , \tag{12}$$

where x is a so-called separation parameter which can be adjusted. The ^{6}Li wave function obtained when harmonic oscillator wave functions represent the α and deuteron clusters, along with the relative motion wave function of Eq. (11), reduces when equal oscillator parameters are used, into the shell model function which describes the lowest configuration $(1s)^4(1p)^2$ in an oscillator potential well.

The remaining wave function was based on a phenomenological α-deuteron cluster model wave function for the ^{6}Li ground state used by Noble,[37]

$$\psi(r) \propto (1 - e^{-r/\rho})^3 e^{-\alpha r}/r . \tag{13}$$

Here α has been defined previously in Eq. (5) and ρ is again an adjustable parameter. This wave function describes correctly the relative motion of the clusters at both large and small separation distances.

The values for the adjustable parameters of Eqs. (10), (11), and (13) were obtained in the following manner. From Eq. (3) it is seen that the ratio of ($\Delta\sigma$/phase space) is proportional to $|\phi(p_R)|^2$. The parameters were adjusted until a best fit was obtained between the theoretical curves for $|\phi(p_R)|^2$ and the experimental data taken with kinematics near that of the free process. Figure 6 shows an example of such a fit for the case in which $\Psi(r)$ was given by Eq. (11). In Eq. (10) λ was determined to be 0.9 ± 0.3 fm^{-1}, the value of the separation parameter x in Eq. (11) was 0.27 ± 0.05, and in Eq. (13) the value for ρ was 0.8 ± 0.2 fm.

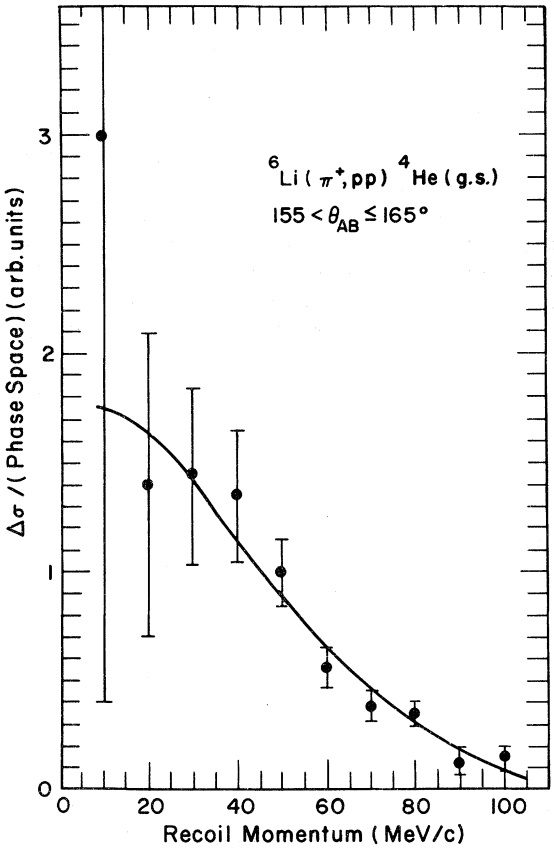

FIG. 6. An example of the fit of $|\phi(p_R)|^2$ based on Eq. (11) to the ($\Delta\sigma$/phase space) distribution for π^+ capture on ^{6}Li which lead to the ground state of ^{4}He.

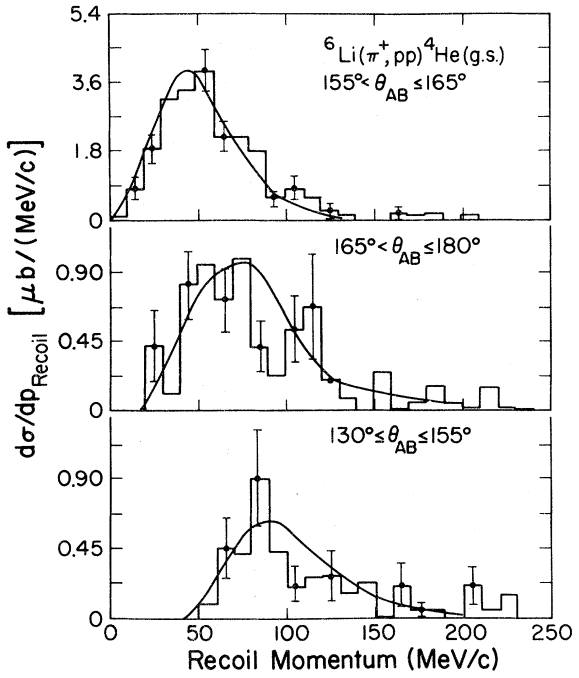

FIG. 7. Experimental distributions in recoil momentum obtained for ^{6}Li$(\pi^+, pp)^4$He(g.s.) events as a function of opening angle region. The curves result from calculations which used the pole model expression of Eq. (4) along with a relative motion wave function of the Hulthen form.

The separation parameter $x = 0.27 + 0.05$ obtained from our data is consistent with values of 0.3 to 0.4 which provide reasonable fits to the elastic charge form factors measured in electron scattering, and to the relative motion form factors measured in the ^{6}Li(π^-, nn)^{4}He reaction.[38]

However, the value for ρ which we obtained is not consistent with the value of 1.4 fm needed to fit the squared charge form factor distribution from electron scattering on ^{6}Li.[37]

It is of interest to compare other predictions of this model with the experimental data in order to test for regions where a breakdown in the applicability of the PWIA may occur. Thus theoretical distributions in interesting kinematical variables have been generated based on the cross section of Eq. (4). Only the distributions in which a Hulthen wave function was used for the cluster relative motion are shown with the data since the distributions obtained with Eqs. (11) and (13) are similar in shape and need not be repeated. Both experimental and theoretical distributions are presented in an unbiased form and have been integrated over the regions defined in Sec. IV. Unless noted otherwise, the comparison is made for data taken with $\theta_B = 98°$. Data and theoretical curves are presented for distributions in the following kinematical variables:

(a) recoil momentum, $\vec{p}_R = \vec{p}_\pi - \vec{p}_A - \vec{p}_B$,
(b) relative momentum, $\vec{p}_{rel} = \vec{p}_A - \vec{p}_B$ (Ref. 39),
(c) Treiman-Yang angle, ϕ_{TY}, and
(d) opening angle, θ_{AB}.

The results of the theoretical calculations and the experimental data for p_R, p_{rel}, and ϕ_{TY} appear in Figs. 7–9. The data are presented for three ranges in opening angle, one corresponding to free-deuteron kinematics ($155° \leq \theta_{AB} < 165°$) and the other two for off-deuteron angle values. The theoretical curves were normalized to the data for events occurring on the free-deuteron opening angle. The pole model is expected to produce the best agreement with the data in this region. This normalization was then used for the other two regions of opening angle ($130° \leq \theta_{AB} < 155°$ and $165° \leq \theta_{AB} \leq 180°$), which are off the kinematics for the free process. This type of comparison serves to

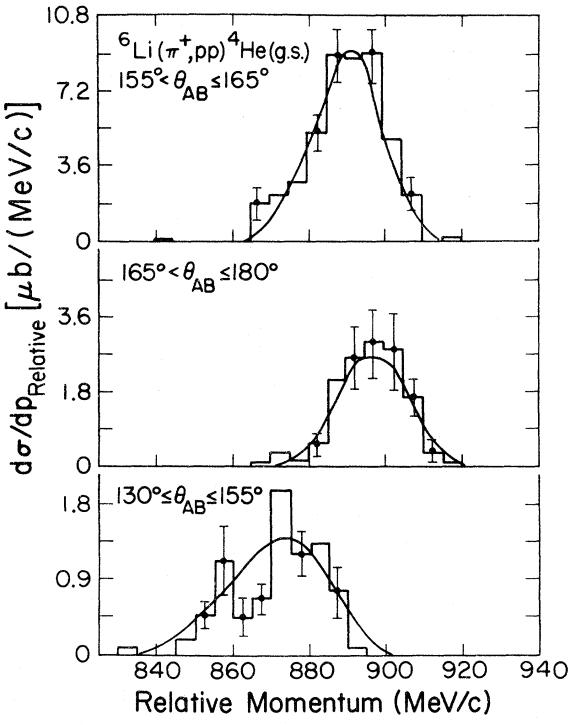

FIG. 8. Distributions in relative momentum for ^{6}Li ground state events with theoretical curves given by the pole model.

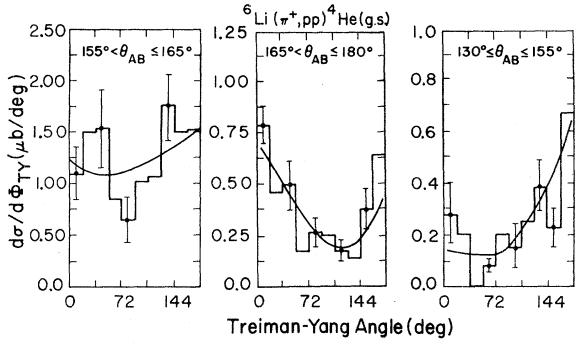

FIG. 9. Treiman-Yang angle distributions for ^{6}Li events leading to the ^{4}He ground state along with curves calculated through the use of Eq. (4).

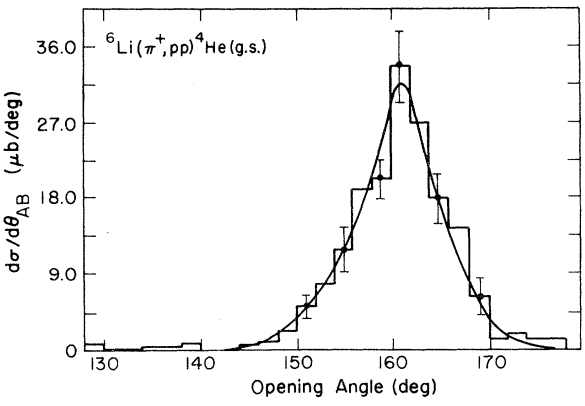

FIG. 10. The opening angle distribution for gound state events with the calculated curve described in Sec. V B 1.

point out regions where the applicability of the pole model may begin to break down.

These figures illustrate that the experimental and theoretical results agree quite well even for events which occur off the free-deuteron opening angle. Further evidence for this agreement appears in Fig. 10, which presents the opening angle distribution for ground state events. The normalization between theory and experiment is the same as that described above. Although our geometrical acceptance allowed us to detect, with good efficiency, events in the range of opening angles from 110 to 180°, most events occur in the region centered at the free-deuteron angle of 161° with a FWHM of 12°.

If the quasideuteron absorption model of Fig. 1 is the dominant reaction mechanism, then the cross section for ground state events should exhibit the same dependence on the c.m. angle as does the free-deuteron cross section. Experimental results are shown in Fig. 11 for various regions of high and low recoil momentum. The dependence of the relative cross section upon the c.m. angle can be fitted well by the function $A(0.23+\cos^2\theta_{\text{c.m.}})$, which is exactly the dependence observed for the free cross section.[26]

From the ratio of the experimental to the theoretical cross section one can obtain the effective number of deuterons in ^{6}Li. The results for events integrated over the regions defined in Sec. IV appear in Table III. Our weighted average value for N_d is 1.25 ± 0.12 which is consistent with the value of 1.55 ± 0.3 obtained by Favier *et al.*[17] The magnitude of N_d for off-deuteron angle setting varies little from the value obtained for on-deuteron kinematics, which again illustrates the applicability of the pole approximation to events which occur off the opening angle for the free process (1). The value of N_d obtained for the ^{6}Li$(\pi^+, pp)^4$He(g.s.) reaction is greater than the value of 0.3 obtained from low energy (p, pd) reactions on ^{6}Li.[40,41] However, a N_d of 0.8 resulted from a measurement of the ^{6}Li$(p, pd)^4$He(g.s.) reaction at 590 MeV.[29] The value of N_d obtained in this experiment of 1.25 is

TABLE III. Experimental and pole model cross sections ^{6}Li data.

θ_A	θ_B	Exp. cross section (−5 to 8 MeV) (μb)	Pole model cross section (μb)	N_d
63	98	143 ±18	118 ± 5	1.21 ±0.15
53	98	135 ±19	114.8 ± 6	1.18 ±0.17
38	98	10.3± 3.1	8.6 ± 1.1	1.193±0.36
78	98	67 ±13.4	59.5 ± 4.2	1.13 ±0.23
42	123	309.7±43	221.75±13.3	1.4 ±0.2
80	80	102.3±16.3	72.7 ± 4.4	1.39 ±0.22

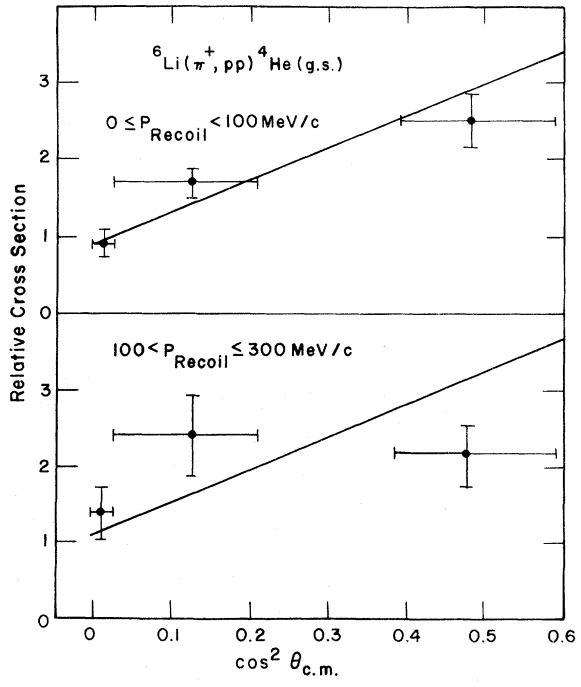

FIG. 11. The c.m. angle dependence for ^{6}Li(π^+, pp)-^{4}He(g.s.) events compared to the $A(0.23+\cos^2\theta_{\text{c.m.}})$ dependence of the free πd cross section.

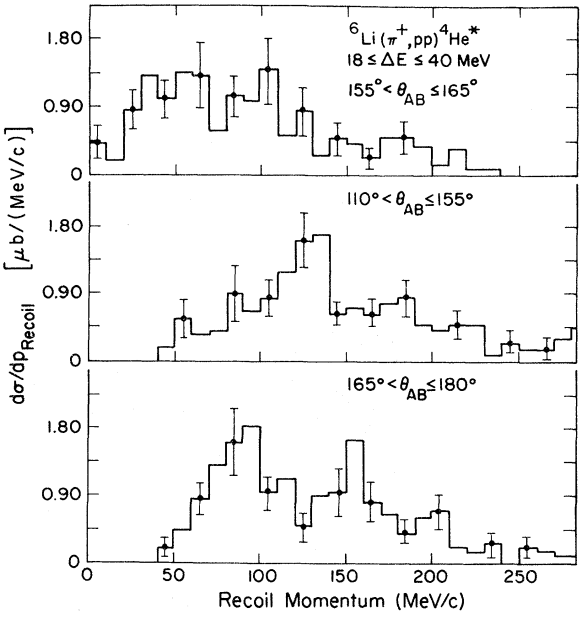

FIG. 12. Recoil momentum distributions as a function of opening angle for ^{6}Li events leading to ^{4}He excited states.

close to the theoretical value of 1 to 1.1 which results from simple shell or cluster model calculations.[38] This indicates that pion absorption reactions are more sensitive to all two-nucleon correlated systems, while knockout reactions select only deuterons.

To summarize our results for ^{4}He ground state events, it has been shown that the theoretical expression for the cross section based on the graph of Fig. 1 describes the general characteristics of the experimental data even for events in opening angle regions off the kinematics of the free process. These distributions, as well as previous measurements of the dependence of the cross section on pion energy,[42] illustrate the importance of the quasideuteron absorption mechanism in the explanation of this process.

2. *^{4}He excited states results*

The higher excitation energy portion of the spectra shown in Fig. 5 peak for the most part around 30 MeV indicating a possible contribution from proposed $T=1$ states of ^{4}He.[43] A smaller contribution to the spectra occurs in the region of 20 MeV, indicating that the $T=0$ states are not as strongly excited in this process.

Figure 12 presents unbiased distributions for recoil momentum shown for three groups of opening angle after integration over the regions described in Sec. IV. The dependence of the cross section on c.m. angle for selected regions of recoil momentum is illustrated in Fig. 13. The events follow, for the most part, the $A(0.23+\cos^2\theta_{\text{c.m.}})$ behavior of the free-deuteron cross section. The opening angle distribution is shown in Fig. 14. Noticeable is the peaking at values of 161–162°, which correspond to the kinematics of reaction (1).

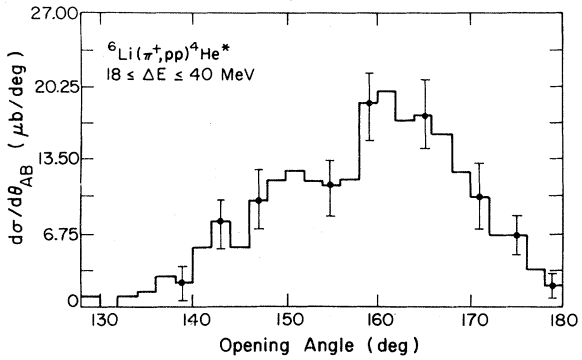

FIG. 14. Opening angle distribution for ^{6}Li(π^+, pp)^{4}He* events.

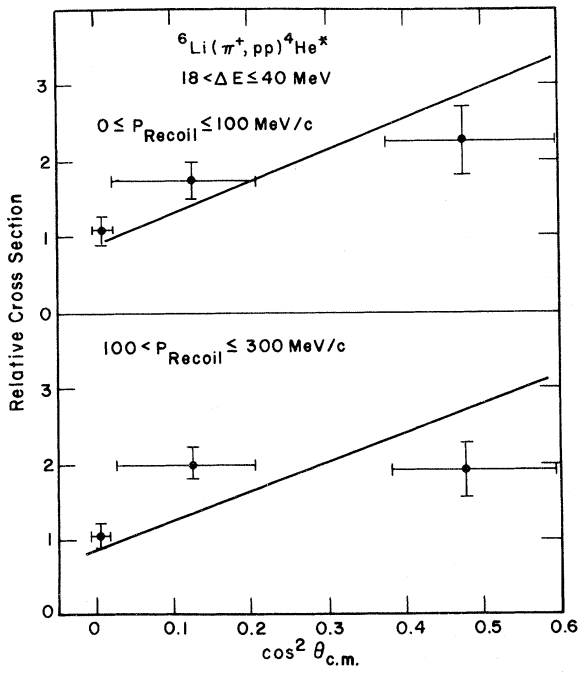

FIG. 13. c.m. angle dependence for ^{6}Li(π^+, pp)^{4}He* events shown as a function of selected regions of recoil momentum. The curves which appear represent the $A(0.23+\cos^2\theta_{\text{c.m.}})$ c.m. dependence of the free πd cross section.

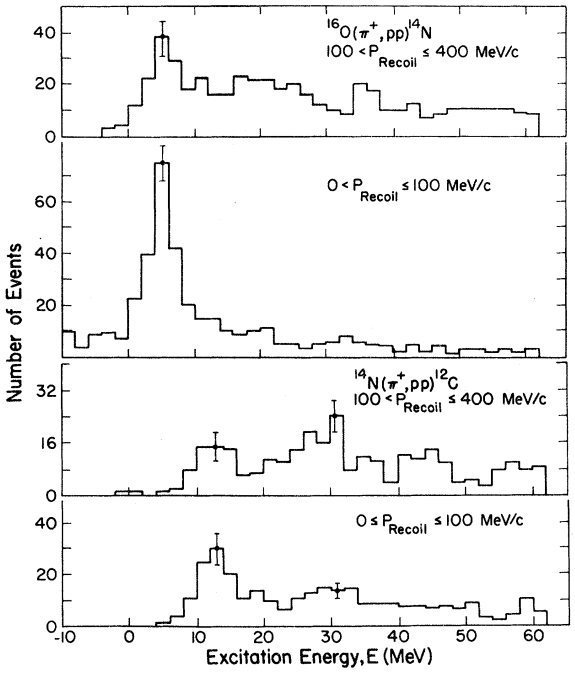

FIG. 15. Excitation energy spectra for ^{16}O(π^+, pp)^{14}N and ^{14}N(π^+, pp)^{12}C events shown for regions of high and low recoil momentum.

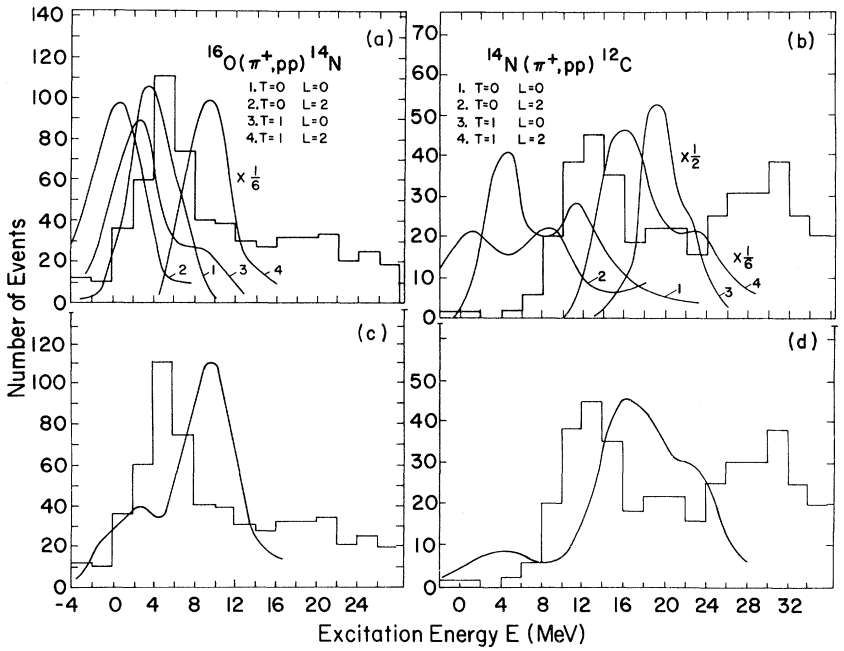

FIG. 16. Excitation energy spectra obtained for (π^+, pp) events on ^{16}O and ^{14}N compared to the fractional parentage calculations of Cohen and Kurath for pickup $A = 16(0, 0)$ and $A = 14(1, 0)$. The upper portion of the figure shows individual curves calculated for the transfer of a singlet or triplet deuteron in an S or D state of orbital angular momentum. The lower part of the figure shows composite curves obtained from these calculations.

The distribution is wider than that obtained for events leading to the ground state of ^{4}He. This may be due in part to events in which absorption takes place on the deuteron cluster and the outgoing protons excite the recoiling α-particle core.

C. Excitation energy spectra from ^{14}N and ^{16}O

The (π^+, pp) reaction on ^{14}N and ^{16}O leads to the excitation energy spectra for the residual ^{12}C and ^{14}N nuclei shown in Fig. 15. Events have been grouped into regions of high and low recoil momentum. The oxygen target data exhibit considerable excitation to states of the residual ^{14}N nuclei in the range 4 to 6 MeV. Little excitation of the ^{14}N ground state is noted. Likewise, the spectra for absorption on the nitrogen target show almost a complete absence of excitation of the ground and first excited states of ^{12}C. In these data two peaks are prominent, the first centered at 12 MeV and the second around 30 MeV. A shell model description of the spectra would attribute the first peak to absorption upon two p-shell nucleons. The second peak may then result from capture on a $(1s, 1p)$ pair.

The excitation energy spectra can be compared with the fractional parentage calculations of Cohen and Kurath[44] in which the wave function for N p-shell nucleons is related to that for $(N-2)$ p-shell nucleons. The two transferred nucleons are coupled to total angular momentum J and isospin T, and may have an orbital angular momentum $l = 0$ or $l = 2$ with respect to the $N-2$ system.

Their results for pickup on $A = 16$ $(J = 0, T = 0)$ and $A = 14$ $(J = 1, T = 0)$ nuclei folded with our resolution function are compared with the experimental data in Fig. 16. In portions 16(a) and 16(b) separate curves representing contributions from the transfer of S and D state singlet and triplet deuterons are shown, while in 16(c) and 16(d) the summed contribution from these curves appear. The excitation energy spectrum of the residual nucleus is best fitted by the fractional parentage curve for the transfer of a triplet deuteron with $L = 0$. The state populated most by this type of transfer is the $J, T = (1, 0)$ state at 3.95 MeV. Since our precision in excitation energy is approximately 0.5 MeV, these results are consistent with our data, which indicates peaking in the excitation energy range from 4 to 6 MeV. These predictions also agree with the results of measurements of the nuclear deexcitation γ rays observed in the reaction $^{16}O(\pi^-, nn)^{14}N$.[45]

The experimental ^{12}C excitation energy spectrum is in poor agreement with the fractional parentage results. The dominant contribution to the calculated spectrum arises from states in the range from

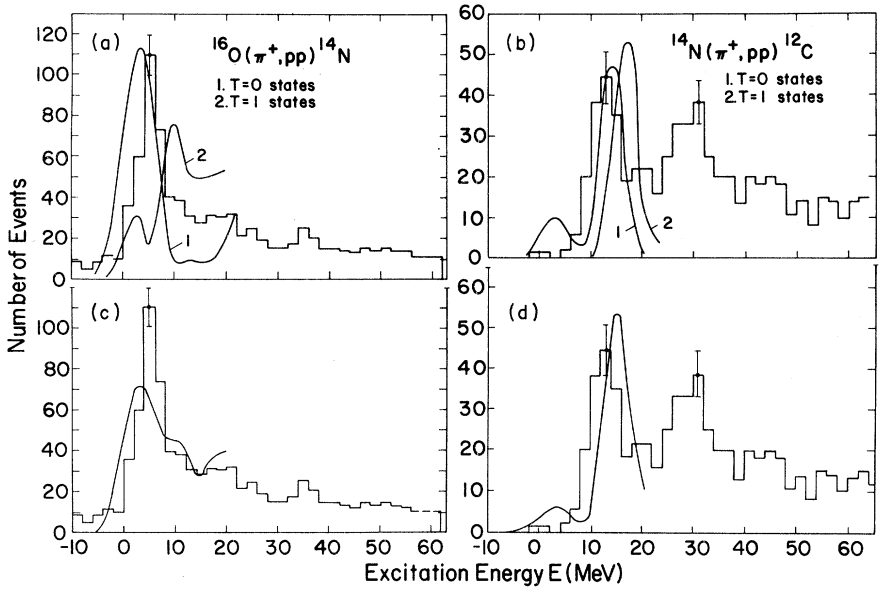

FIG. 17. Same as Fig. 16, except comparison is made to the calculations of Kopaleishvili. The lower parts of the figure again represent the composite curves obtained from a combination of the curves shown in the upper part of the figure.

14 to 18 MeV, compared to the experimental peak between 10 and 16 MeV. Also, the prediction of a strong transition to the 4.43-MeV state of ^{12}C from the transfer of a triplet deuteron with $l=0$ fails to agree with the data since we see little evidence of such a transition.

In Fig. 17 the spectra are compared with the theoretical predictions of Kopaleishvili *et al.*[46] for excitation of $T=0$ and $T=1$ states of the residual ^{14}N and ^{12}C nuclei. The calculations are for 100-MeV pions and assume capture on two p-shell nucleons. A fractional parentage decomposition based on intermediate coupling of the p-shell nucleons was used, and final state interactions between the outgoing protons were included.

According to this calculation, the ground and 3.95-MeV state of ^{14}N would be most strongly excited. Our results are consistent with strong excitation of the ^{14}N first excited state. For the $^{14}N(\pi^+, pp)^{12}C$ reaction, the calculation indicates moderate excitation of the 4.4-MeV state with strong excitation predicted for states in the range from 14 to 16 MeV. Our data show peaking around 13 MeV with little excitation below 6 MeV. We have used the PWIA to generate theoretical distributions to compare with the experimental data in regions of low-lying excitations. To describe the quasideuteron on which capture occurs, the shell model and fractional parentage decomposition of Balashov, Boyarkina, and Rotter [47] was used to calculate the fragmentation of a nucleus A into a state (E, J, T) of the residual nucleus and a quasideuteron. The quasideuteron is assumed to be composed of two p-shell nucleons and can be in a S or D state in orbital angular momentum with respect to the $A-2$ system. The Fourier transform squared includes both $l=0$ and $l=2$ contributions and has the form

$$|\phi(p_R)|^2 = \alpha_0 |\phi(p_R)|^2 + \alpha_2 |\phi_2(p_R)|^2 . \tag{14}$$

The quantities α_0 and α_2 are the probabilities for $l=0$ and $l=2$ transfer. The terms $\phi_0(p_R)$ and $\phi_2(p_R)$ are given by[48]

$$|\phi_0(p_R)|^2 = \frac{1}{4\pi}\frac{6}{\sqrt{\pi}}\frac{1}{p_0^3}[1-\tfrac{2}{3}(p_R/p_0)^2]^2 \times \exp[-(p_R/p_0)^2], \tag{15}$$

$$|\phi_2(p_R)|^2 = \frac{1}{4\pi}\frac{16}{15\sqrt{\pi}}\frac{1}{p_0^3}(p_R/p_0)^4 \times \exp[-(p_R/p_0)^2] \tag{16}$$

TABLE IV. Values obtained for the adjustable parameters appearing in Eq. (14) after fits to the ($\Delta\sigma$/phase space) distributions for ^{16}O and ^{14}N events.

	α_0	α_2	p_0 (MeV/c)
^{16}O	$0.66^{+0.07}_{-0.01}$	$0.34^{+0.02}_{-0.06}$	180^{+30}_{-20}
^{14}N	$0.65^{+0.01}_{-0.01}$	$0.35^{+0.01}_{-0.01}$	180^{+20}_{-15}

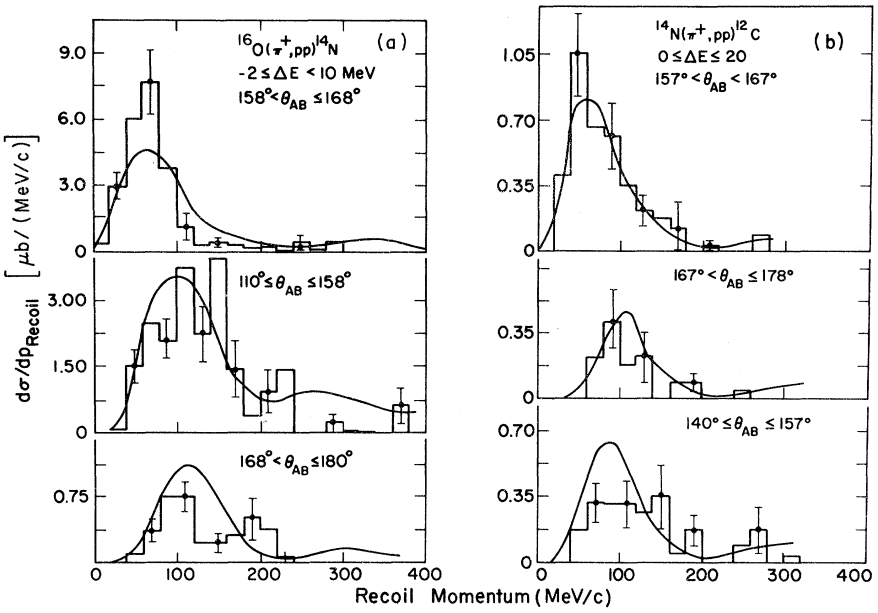

FIG. 18. (a) Recoil momentum distributions as a function of opening angle for π^+ absorption on ^{16}O which lead to low-lying states of the residual ^{14}N nucleus. The curves were calculated using the PWIA expression of Eq. (3) as described in Sec. V C. (b) Recoil momentum distributions for the nitrogen target data.

and are normalized such that

$$\int |\phi_l(p_R)|^2 d^3p = 1 \quad (l = 0, 2). \tag{17}$$

The quantity p_0 is related to the harmonic oscillator frequency

$$p_0 = (\hbar \mu \omega)^{1/2}, \tag{18}$$

where μ is the reduced mass of the deuteron.

The values for α_0, α_2, and p_0 were obtained in a manner similar to that used to fit the adjustable parameters in the ^{6}Li data. That is, the expression for $|\phi(p_R)|^2$ given by Eq. (14) was fitted to the ($\Delta\sigma$/phase space) distribution for the oxygen and nitrogen events of interest.

The values for α_0, α_2, and p_0 were found to be almost identical for the two nuclei and appear in Table IV. The harmonic oscillator length parameter r_0 can be determined from the relationship $p_0 r_0 = \hbar$, and for $p_0 = 180$ MeV/c a value of $r_0 = 1.1^{+0.13}_{-0.2}$ fm is obtained. The value of r_0 that we measure is the harmonic oscillator parameter for the c.m. motion of a pair of nucleons which must be multiplied by $\sqrt{2}$ in order to compare it with the single-particle parameter as measured, e.g., in electron scattering. Electron scattering data give values of r_0 for ^{16}O of 1.76 fm and 1.6 fm for ^{14}N [49] which should be compared with $\sqrt{2} \times 1.1$ fm $= 1.55$ fm from our data. The agreement for these nuclei is surprisingly good considering the limitations of the PWIA.

D. Results–oxygen events leading to ^{14}N excitation near 5 MeV

In Fig. 18(a) appear distributions in recoil momentum for oxygen target events occurring in three opening angle ranges; one corresponding to deuteron kinematics ($158° < \theta_{AB} \le 168°$) and the others to values on either side. These results are for events occurring in the excitation energy range

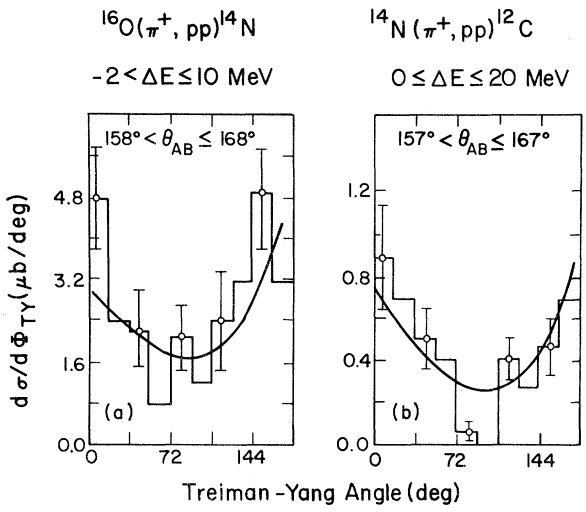

FIG. 19. Treiman-Yang angle distributions for (a) ^{16}O and (b) ^{14}N target events with PWIA predictions for on-deuteron kinematics.

from −2 to 10 MeV. Integration has been performed over the regions described in Sec. IV for apparatus settings in which $\theta_B = 113°$. Theoretical curves normalized to the data in the opening angle range $158° < \theta_{AB} \leq 168°$ and calculated using Eqs. (14)–(16) with the parameters appearing in Table IV are also shown. In Fig. 19(a) the Treiman-Yang angle distribution for oxygen target events for on-deuteron kinematics appears. Agreement between the experimental results and the PWIA theoretical distributions is good since the general characteristics of the data are reproduced by the curves even for opening angles off the kinematics for reaction (1). A distribution in opening angle is shown in Fig. 20(a). The distribution has a FWHM of 22°, and although wider than that characterizing the ^{6}Li ground state events, is fitted well by the PWIA calculations. Figure 21 shows that the dependence of the cross section of these events generally follows the $A(0.23 + \cos^2\theta_{c.m.})$ dependence of the free-deuteron cross section although some disagreement occurs for events which have high values of recoil momentum.

The effective number of deuterons in ^{16}O obtained as a function of opening angle appear in Table V. The listed cross sections have been integrated over the regions described in Sec. IV A. Balashov *et al.*[47] calculated a value of 7.0 for the effective number of deuterons for excitation of the 3.95 and 5.1 MeV levels of ^{14}N and a value of 11.6 if a level at 11.5 MeV is included. These values include both $l = 0$ and $l = 2$ transfer. These results are consistent with the weighted average value for N_d of 10 ± 1.1 obtained in this experiment. Favier *et al.*[17] obtained an estimate of the effective number of deuterons in ^{16}O from the ratio of the ^{14}N cross section from 0 to 20 MeV excitation to the free-

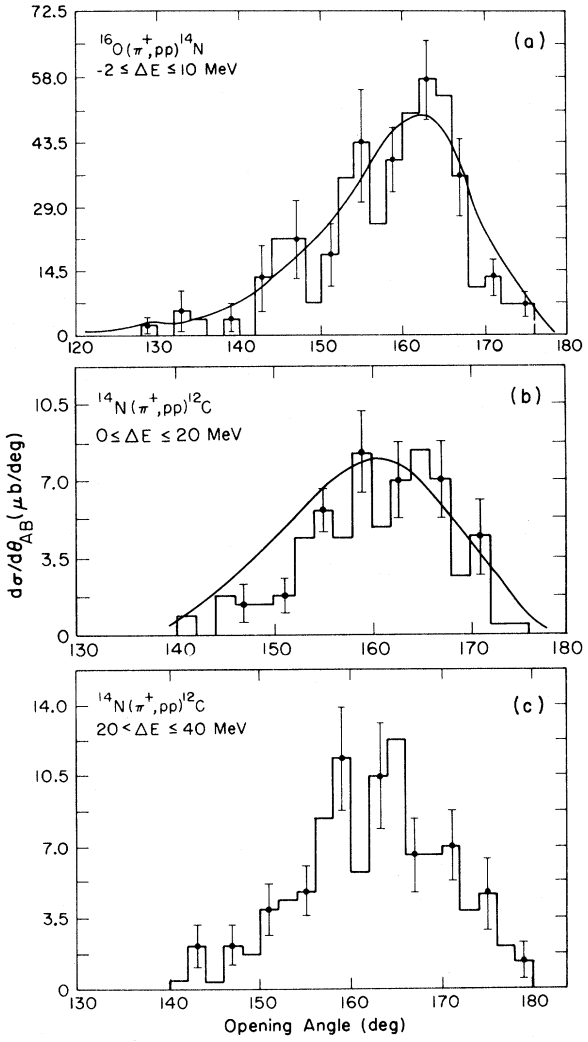

FIG. 20. (a) The opening angle distribution for $^{16}O(\pi^+, pp)$ events leading to low values of excitation of ^{14}N. Also shown is the curve obtained from the PWIA. In part (b) a similar distribution is shown for $^{14}N(\pi^+, pp)$ events leading to ^{12}C excitation from 0 to 20 MeV. Also shown is the PWIA curve for these events. The opening angle distribution for nitrogen target events leading to ^{12}C excitations from 20 to 40 MeV appears in part (c).

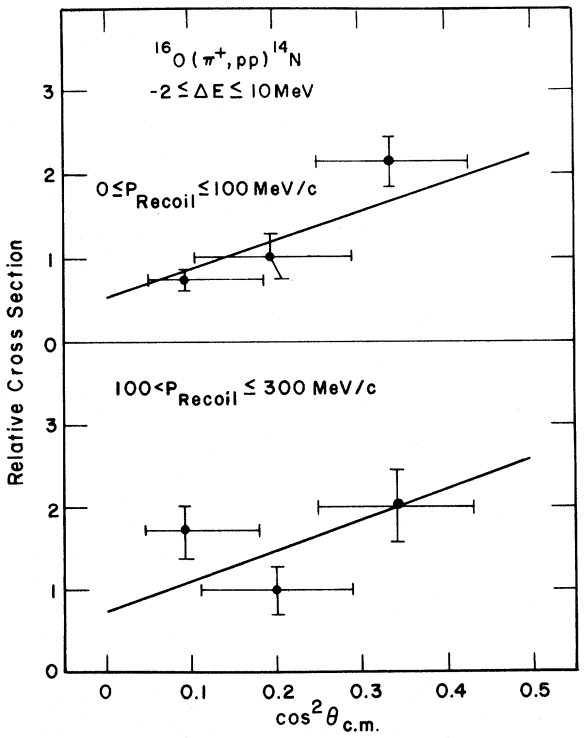

FIG. 21. c.m. angle dependence for selected ^{16}O-$(\pi^+, pp)^{14}N$ events. The curves show the $A(0.23 + \cos^2\theta_{c.m.})$ dependence of the $\pi^+ + d \rightarrow p + p$ cross section.

TABLE V. Experimental and PWIA cross sections for ^{16}O and ^{14}N data.

θ_A	θ_B	Exp. cross section (μb)	PWIA cross section (μb)	N_d
		^{16}O$(\pi^+, pp)^{14}$N ($-2 \leq \Delta E \leq 10$ MeV)		
50	113	279 ±42	30.3 ±1.5	9.2±1.6
100	61	231.2±46	21.88±1.1	10.5±2
25	113	158.9±52	14.2 ±1.2	11.2±3.6
65	113	148 ±49	17.38±1.5	8.7±2.8
37.5	113	32.3± 7.8	2.96±0.2	10.9±2.6
		^{14}N$(\pi^+, pp)^{12}$C ($0 \leq \Delta E \leq 20$ MeV)		
80	80	131 ±20	23.4 ±1.5	5.6±1

deuteron cross section; their value, $N_d = 2$, is in disagreement with the results of this experiment.

E. Nitrogen results

Theoretical and experimental distributions in recoil momentum and Treiman-Yang angle for nitrogen target events leading to ^{12}C excitations from 0 to 20 MeV appear in Figs. 18(b) and 19(b). Even though the experimental uncertainties are large, there is general agreement between the experimental results and the theoretical calculations. The opening angle distribution, shown in Fig. 20(b), is centered at the value (160°) for the kinematics of process (1) and has a width comparable to the oxygen data of Sec. V E.

In Table V the cross section is given for absorption on ^{14}N leading to ^{12}C excitations from 0 to 20 MeV integrated over the region defined in Table I. Also presented are the calculated PWIA cross section results and the value for the effective number of deuterons in ^{14}N. This value, $N_d = 5.6 \pm 1$, is in contrast to the result of 0.8 obtained by Balashov *et al.*[47] from the sum over contributions from $T = 0$ levels which lie below 20 MeV. One cause of the difference may result from the fact that in the calculation of Balashov only $l = 0$ transfers were included. In our experiment, however, we had to include some $l = 2$ contribution in the theoretical curves to obtain agreement with the experimental data. Again, our value of N_d disagrees with that from the experiment of Favier *et al.*[17] who obtained a value of 0.7 through the method described in the previous section.

For events leading to ^{12}C excitation energies from 20 - to 40-MeV distributions in recoil momentum, Treiman-Yang angle, etc., were found to have generally the same shape as those described for ^{12}C excitations in the range from 0 to 20 MeV. The unbiased distribution in opening angle obtained for events in peak 2 of the nitrogen target data after integration over the region defined in Table I appears in Fig. 20(c). Again the peak of the opening angle distribution occurs at the angle for absorption on a free deuteron.

VI. SUMMARY AND GENERAL CONCLUSIONS

Our examination of the (π^+, pp) process on the nuclei ^{6}Li, ^{14}N, and ^{16}O has shown general agreement between data occurring in the low-lying states of the residual nucleus and the predictions of the PWIA. With the value of the parameters given in Sec. V B 1, good agreement was found between the data from the ^{6}Li$(\pi^+, pp)^4$He(g.s.) reaction and the theoretical predictions. The agreement was consistent for all experimental distributions, both on the free-deuteron kinematics and off. These events were shown to follow the $A(0.23 + \cos^2\theta_{\text{c.m.}})$ dependence of the free-deuteron cross section, an observation which requires the angular coverage of the present experiment. Values of the effective number of deuterons were consistent with previous results. It was possible to describe completely our data in terms of only two parameters, one related to the wave function used to describe the relative motion of the clusters and the other being the value for the effective number of deuterons N_d.

The analysis of (π^+, pp) events occurring on ^{14}N and ^{16}O illustrate that the structure of these nuclei has a marked influence on the levels of the residual nucleus which will be excited. A general feature of the spectra was the absence of excitations leading to the ground state, in contrast to the fractional parentage results.

After suitable adjustment of the harmonic oscillator length parameters, general agreement was obtained between the theoretical curves of the PWIA and the experimental distributions restricted to low values of excitation in the residual nucleus. The harmonic oscillator length parameter for ^{14}N agreed well with that obtained from electron scattering data. Oxygen target events leading to states in ^{14}N around 4 to 6 MeV exhibited the same general dependence upon c.m. angle as the free-deuteron cross section. For the oxygen and nitrogen target data, events leading to low-lying states of the residual nucleus had opening angle distributions which peaked around the kinematics for absorption on a free deuteron.

These results illustrate the significance of the two-nucleon absorption mechanism given by the pole model or PWIA in describing the data presented here. However, in order to obtain information concerning short-range correlations from the study of this reaction, more complete theoretical descriptions, which include short-range correlations and distortions in an explicit manner, are needed.

ACKNOWLEDGMENTS

We acknowledge valuable conversations with E. Lomon, W. Gibbs, B. Goplin, and J. M. Eisenberg, and the contributions made by P. D. Barnes during various stages of the experiment. Also appreciated were the assistance and cooperation of the Lawrence Berkeley Laboratory 184-inch synchrocyclotron crew. Special thanks are given to R. Rajala and C. Dalton for their assistance during the setup and operation of the experimental equipment. One of us (EDA) acknowledges financial support from Associated Western Universities, Incorporated, for the duration of the experiment.

---

*Work performed under the auspices of the U.S. Atomic Energy Commission.

†Present address: Los Alamos Scientific Laboratory, Los Alamos, New Mexico 87544.

‡Present address: Virginia Polytechnic Institute and State University, Blacksburg, Virginia 24061.

§Present address: Oregon State University, Corvallis, Oregon 97311.

‖Present address: Upsala College, East Orange, New Jersey 07019.

[1]T. Ericson, Phys. Lett. 2, 278 (1962); in *Proceedings of the Conference on Direct Interactions and Nuclear Reaction Mechanisms, Padua, 1962,* edited by E. Clementel and C. Villi (Gordon and Breach, London, 1963).

[2]M. Jean, in *Proceedings of the Conference on Direct Interactions and Nuclear Reaction Mechanisms, Padua, 1962* (see Ref. 1).

[3]J. M. Eisenberg and J. LeTourneux, Nucl. Phys. B3, 47 (1967).

[4]T. I. Kopaleishvili, Yad. Fiz. 4, 538 (1966) [transl.: Sov. J. Nucl. Phys. 4, 382 (1967)].

[5]D. S. Koltun and A. Reitan, Phys. Rev. 141, 1413 (1966); 155, 1139 (1967); Nucl. Phys. B4, 629 (1968).

[6]W. Elsaesser and J. M. Eisenberg, Nucl. Phys. A144, 44 (1970).

[7]R. I. Jibuti and T. I. Kopaleishvili, Nucl. Phys. 55, 337 (1964).

[8]T. I. Kopaleishvili, Nucl. Phys. B1, 335 (1967).

[9]S. G. Eckstein, Phys. Rev. 129, 413 (1963).

[10]P. P. Divakaran, Phys. Rev. 139, B387 (1965).

[11]R. Guy, J. M. Eisenberg, and J. LeTourneux, Nucl. Phys. A112, 689 (1968).

[12]R. S. Kaushal and Y. R. Waghmare, Phys. Lett. 31B, 637 (1970).

[13]C. Morris and H. J. Weber, Ann. Phys. (N.Y.) 79, 34 (1973).

[14]V. M. Kolybasov and T. A. Lomonsova, Yad. Fiz. 11, 578 (1970) [transl.: Sov. J. Nucl. Phys. 11, 325 (1970)].

[15]G. Alberi and L. Taffara, Nuovo Cimento 58B, 441 (1968).

[16]R. L. Burman and M. E. Nordberg, Phys. Rev. Lett. 2, 229 (1968).

[17]J. Favier, T. Bressani, G. Charpak, L. Massonnet, W. E. Meyerhof, and C. Zupanicic, Nucl. Phys. A169, 540 (1971).

[18]C. E. Swannack, Carnegie-Mellon University Report No. CAR-882-27, 1971.

[19]M. Jain, P. G. Roos, H. G. Pugh, and H. D. Holmgren, Nucl. Phys. A153, 99 (1970).

[20]E. D. Arthur, Los Alamos Scientific Laboratory Report No. LA-5230-T, 1973.

[21]J. Amato, R. L. Burman, R. Macek, J. Oostens, W. Shlaer, E. Arthur, S. Sobottka, and W. C. Lam, Phys. Rev. C 9, 501 (1974).

[22]D. F. Measday and C. Richard-Serre, Nucl. Instrum. Methods 76, 45 (1969).

[23]J. N. Palmieri and J. Wolfe, Nucl. Instrum. Methods 76, 55 (1969).

[24]S. B. Treiman and C. N. Yang, Phys. Rev. Lett. 8, 140 (1962).

[25]I. S. Shapiro, Usp. Fiz. Nauk 92, 549 (1967) [transl.: Sov. Phys. Usp. 10, 515 (1968)]; *Interaction of High-Energy Particles with Nuclei, Proceedings of the International School of Physics "Enrico Fermi," Course XXXVIII,* edited by T. E. O. Ericson (Academic, New York, 1967), p. 210.

[26]C. M. Rose, Phys. Rev. 154, 1305 (1967).

[27]H. Davies, H. Muirhead, and S. N. Woulds, Nucl. Phys. 78, 673 (1966).

[28]F. Calligaris, C. Cernigoi, I. Gabrielli, and F. Pellegrini, Nucl. Phys. A126, 242 (1969).

[29]J. C. Alder, W. Pollhopf, W. Kossler, C. F. Perdrisat, W. K. Roberts, P. Kitching, G. A. Moss, W. C. Olsen, and J. R. Priest, Phys. Rev. C 6, 18 (1972).

[30]I. A. Mackenzie, S. F. Mark, and T. Y. Li, Nucl. Phys. A178, 225 (1971).

[31]J. R. Pizzi, M. Gaillard, A. Guichard, M. Gusakow, G. Reboulet, and C. Ruhla, Nucl. Phys. A136, 496 (1969).

[32]N. F. Golovanova and N. S. Zelenskaya, Yad. Fiz. 8, 274 (1968) [transl.: Sov. J. Nucl. Phys. 8, 158 (1969)].

[33]C. Richard-Serre, W. Hirt, D. F. Measday, E. G. Michaelis, M. J. M. Saltmarsh, and P. Skarek, Nucl. Phys. B20, 413 (1970).

[34]Y. C. Tang, K. Wildermuth, and L. D. Pearlstein, Phys. Rev. 123, 548 (1962).

[35]S. C. Park and J. P. Rickett, Phys. Rev. C 3, 1926 (1971).

[36]Y. Sakamoto, Nuovo Cimento 37, 774 (1965).

[37]J. V. Noble, Phys. Rev. C 9, 1209 (1974).

[38]Yu. A. Kudeyarov, I. V. Kurdyumov, V. G. Neudatchin, and Uy. F. Smirnov, Nucl. Phys. A163, 316 (1971).

[39]Our definition of relative momentum is actually twice the value normally defined, i.e., $\frac{1}{2}(\vec{p}_A - \vec{p}_B)$.

[40]R. B. Liebert, K. H. Purser, and R. L. Burman, Nucl. Phys. A216, 335 (1973).

[41]C. L. Ruhla, M. Riou, J. P. Garron, J. C. Jacmart, and L. Massonnet, Phys. Lett. 2, 44 (1962).

[42]T. Bressani, G. Charpak, J. Favier, L. Massonnet, W. E. Meyerhof, and C. Zupancic, Nucl. Phys. B9, 427 (1969).

[43]W. E. Meyerhof and T. A. Tombrello, Nucl. Phys. A109, 1 (1968).

[44]S. Cohen and D. Kurath, Nucl. Phys. A141, 145 (1970).
[45]W. J. Kossler, H. O. Funsten, B. A. MacDonald, and W. F. Lankford, Phys. Rev. C 4, 1551 (1971).
[46]T. I. Kopaleishvili, I. Z. Machabeli, G. Sh. Gogsadze, and N. B. Krupennikova, Yad. Fiz. 7, 292 (1968) [transl.: Sov. J. Nucl. Phys. 7, 198 (1968)].
[47]V. V. Balashov, A. N. Boyarkina, and I. Rotter, Nucl. Phys. 59, 417 (1964).
[48]J. R. Pizzi, Ph.D. thesis, University of Lyon, 1970 (unpublished).
[49]L. R. B. Elton, *Nuclear Sizes* (Oxford U. P., London, 1961).